Phosphorus Heterocycles

International Edition: DOI: 10.1002/anie.201605963
German Edition: DOI: 10.1002/ange.201605963

# A Stable Crystalline Triarylphosphine Oxide Radical Anion

*Tobias A. Schaub, Eva M. Zolnhofer, Dominik P. Halter, Tatyana E. Shubina, Frank Hampel, Karsten Meyer, and Milan Kivala**

***Abstract:*** *Triarylphosphine oxides ($Ar_3P{=}O$) are being intensely studied as electron-accepting (n-type) materials. Despite the widespread application of these compounds as electron conductors, experimental data regarding the structural and electronic properties of their negatively charged states remain scarce owing to their propensity for follow-up chemistry. Herein, a carefully designed triarylphosphine oxide scaffold is disclosed that comprises sterically demanding spirofluorenyl moieties to shield the central phosphoryl (P=O) moiety. This compound undergoes chemical one-electron reduction to afford an exceptionally stable radical anion, which was isolated and characterized by X-ray crystallography for the very first time. The experimental data, corroborated by computational studies, shall allow for the construction of phosphine oxide materials with enhanced stability.*

Owing to the unique bonding situation at the pentavalent phosphorus center, the phosphoryl moiety acts as an electron-accepting unit.[1] The formal double bond in the P=O fragment is significantly polarized and most appropriately described in terms of so-called negative hyperconjugation, that is, the π back-donation from the lone pair at oxygen into the antibonding σ* orbital localized at phosphorus.[2,3] These characteristics render the phosphoryl moiety a valuable building block for the construction of versatile electron acceptors, an aspect of vital importance in the context of the vigorously developing field of organic electronics.[4] Triarylphosphine oxides have emerged as a promising class of electron-conducting (n-type) materials particularly suited for application in phosphorescent organic light-emitting diodes,[5] owing to their superior electron-transport ability, favorable morphological stability, and high triplet energy.[6] Although triarylphosphine oxides appear to meet almost all of the key requirements to serve as ideal n-type semiconductors, their chemical instability during operation has recently been identified as detrimental to the device lifetime.[7,8] The observed device decay mostly originates from the considerably lowered P–C($sp^2$) bond dissociation energies in the negatively charged states, which are actively involved in the electron transport.[7] In fact, initial research activities on the electrochemical[9,10] and chemical reduction of triarylphosphine oxides with alkali metals date back to the 1950s[11–13] and were most likely conducted because of chemical curiosity in analogy to the ketyl radical anion.[14] These early studies were mainly based on electron paramagnetic resonance (EPR) analysis of the one-electron reduced triarylphosphine oxides, which indicated that the unpaired electron spin density is distributed over the adjacent phenyl moieties.[9,10] However, the formed radical anions were prone to subsequent chemical reactions that led to numerous paramagnetic and non-paramagnetic secondary products, which hampered their isolation and characterization in the solid state.[11–13,15] Apart from these early spectroscopic studies and theoretical calculations later on,[16] to the best of our knowledge, no structural information regarding triarylphosphine oxide radical anions that is based on X-ray crystallographic analysis has been reported to date.

In light of the continuously growing significance of organic phosphine oxide materials, structural characterization of the corresponding anionic radical species in the solid state would be highly desirable as it could provide data essential for the molecular design of phosphine oxide scaffolds with enhanced stability. To this end, it is crucial to stabilize the vulnerable P–C($sp^2$) bonds in the negatively charged species by sufficient steric protection of the phosphorus-centered radicals. Both requirements can be fulfilled by embedding the phosphorus atom in a π-conjugated polycyclic system akin to the previously reported dimethylmethylene-bridged phosphine **A**[17] and its oxygen-[18] and sulfur-bridged[19] phosphine oxide analogues **B1** and **B2** (Figure 1).

With this in mind, we synthesized triarylphosphine oxide scaffold **1**, in which the bridging C($sp^3$) spiro junctions are decorated with rigid fluorenyl moieties to sterically protect

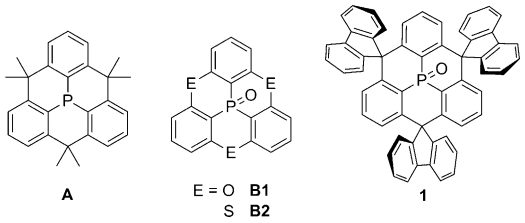


***Figure 1.*** Bridged triarylphosphine **A**[17] and triarylphosphine oxides **B1**[18] and **B2**,[19] which were reported previously. The spirofluorene-bridged scaffold **1** synthesized in this work.

[*] T. A. Schaub, Dr. F. Hampel, Dr. M. Kivala
Chair of Organic Chemistry I
Department of Chemistry and Pharmacy
University of Erlangen-Nürnberg
Henkestrasse 42, 91054 Erlangen (Germany)
E-mail: milan.kivala@fau.de
E. M. Zolnhofer, D. P. Halter, Prof. Dr. K. Meyer
Chair of General and Inorganic Chemistry
Department of Chemistry and Pharmacy
University of Erlangen-Nürnberg
Egerlandstrasse 1, 91058 Erlangen (Germany)
Dr. T. E. Shubina
Computer Chemistry Center (CCC)
University of Erlangen-Nürnberg
Nägelsbachstrasse 25, 91052 Erlangen (Germany)

Supporting information for this article can be found under: http://dx.doi.org/10.1002/anie.201605963.

 © 2016 Wiley-VCH Verlag GmbH & Co. KGaA, Weinheim 

the central phosphoryl moiety. We demonstrate that **1** undergoes chemical reduction to the corresponding radical anion $\mathbf{1}^{\bullet-}$ with unique stability, which enabled the isolation and X-ray crystallographic characterization of the negatively charged state of a triarylphosphine oxide for the very first time. Experimental and computational studies revealed the peculiar electronic situations in **1** and its anionic state $\mathbf{1}^{\bullet-}$, which result from the steric constraint around the phosphoryl moiety.

As shown in Scheme 1, complete lithiation of tris(2-bromophenyl)phosphine (**2**)[20] with *t*-BuLi in $Et_2O$/THF at

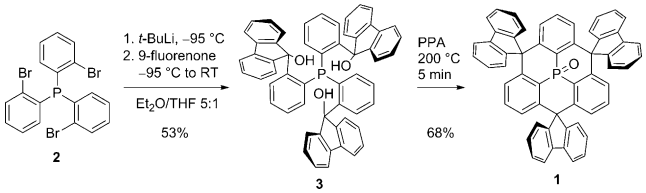


***Scheme 1.*** Synthesis of phosphine oxide **1**. PPA = polyphosphoric acid, THF = tetrahydrofuran.

−95 °C resulted in a yellow solution, which was stable for a few hours at this temperature. The lithiated species reacted readily with 9-fluorenone to afford **3** in 53% yield on gram scale (for X-ray structural analysis and the properties of **3**, see the Supporting Information). The final intramolecular Friedel–Crafts cyclization was achieved upon treatment of **3** with polyphosphoric acid at 200 °C for 5 min to deliver the trispirocyclic phosphine oxide **1** as a white microcrystalline solid in 68% yield after purification by column chromatography. The harsh reaction conditions were found to be crucial for the formation of **1** as at lower temperatures, the reaction times were significantly prolonged, and below 150 °C, only partially cyclized products were identified in the reaction mixture. Interestingly, the $^{31}$P NMR (162.0 MHz, $CD_2Cl_2$) resonance of **1** was dramatically upfield-shifted to −21.0 ppm compared to that of non-bridged triphenylphosphine oxide ($Ph_3PO$; $\delta = 27.5$ ppm).

X-ray crystallographic analysis of single crystals obtained by slow evaporation of an ethyl acetate solution of **1** at room temperature (RT) revealed that the triarylphosphine oxide core adopts a bowl-shaped structure with a bowl depth of 1.50 Å, which is surrounded by the three perpendicular fluorenyl flanks (Figure 2).[21] The steric congestion at the

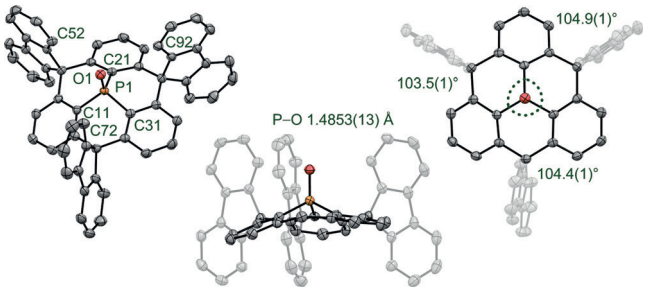


***Figure 2.*** X-ray crystal structure of **1**. Thermal ellipsoids set at 50% probability. Hydrogen atoms and solvent molecules omitted for clarity.

phosphorus center in **1** is reflected in the shortened average P–C bond of 1.762(2) Å compared to that of $Ph_3PO$ (1.803(1) Å; Table 1).[22] The phosphorus center in **1** is also

***Table 1:*** Selected bond lengths [Å] and angles [°] of neutral **1** and the radical anion $\mathbf{1}^{\bullet-}[K\subset 18\text{-crown-}6]^+$ obtained from X-ray crystallographic analysis (top) and theoretical calculations (bottom, in italics; see the Supporting Information).

| | P–$C_{av}$[a] | P–O | ΣC-P-C | Bowl depth[21] |
|---|---|---|---|---|
| **1** | 1.762(2) | 1.4853(13) | 312.8(3) | 1.50 |
| | *1.759(2)* | *1.487* | *310.2* | *1.60* |
| $\mathbf{1}^{\bullet-}$ | 1.747(4) | 1.492(3) | 308.7(6) | 1.71 |
| | *1.752* | *1.501* | *305.8* | *1.79* |

[a] Average values are shown with standard deviations calculated according to: $\{\Sigma(x_i-\langle x\rangle)^2/(n-1)\}^{1/2}$.

characterized by increased pyramidalization, with the sum of the C-P-C angles being 312.8(3)° ($Ph_3PO$: 318.6(3)°).[22] The bridging fluorenyl moieties are bent towards the phosphoryl unit, indicating an intramolecular hydrogen-bond interaction, C($sp^2$)–H···O, with an average C52/72/92···O1 distance of 3.21(6) Å. The observed elongation of the P–O bond in **1** (1.4853(13) Å) compared to $Ph_3PO$ (1.479(2) Å)[22] indicates a slight weakening of this bond. However, a direct assessment of the P–O bond strength in **1** in comparison to that of $Ph_3PO$ by means of infrared spectroscopy was not possible owing to the pronounced dependency of the $\nu$(P–O) stretching frequency on the environment,[23] that is, on the extent of intermolecular interactions in solution and in the solid state (see the Supporting Information).

For a better understanding of the structural and electronic characteristics of **1**, density functional theory (DFT) calculations at the PBE0/def2-QZVP level of theory were carried out. In the optimized structure of **1**, all of the P–C and P–O bond lengths are in good agreement with those determined by X-ray crystallography (Table 1). To elucidate the considerable shielding of the phosphorus center, population, natural bond orbital (NBO), natural localized molecular orbital (NLMO), atoms in molecules (AIM), and electron localization function (ELF) studies were conducted, which all confirmed the presence of negative hyperconjugation at the P–O moiety (see the Supporting Information).[1–3] The AIM analysis showed that the bond critical point (bcp) of the P–O bond is shifted towards the phosphorus atom, with a P–bcp distance of 0.88 Å and an O–bcp distance of 0.61 Å, and is characterized by a positive Laplacian electron density ($\nabla^2\rho$) as well as a negative electronic energy density, which is in agreement with previous results (Figure S35a).[24] Moreover, Mayer's bond order of **1** is reduced to 1.59–1.76 ($Ph_3PO$: 2.05–2.10) depending on the level of theory. Reduced density gradient analysis clearly illustrates the weak intramolecular C($sp^2$)–H···O interaction (Figure S35b). Together with the anisotropy of the induced current density (ACID) plot (Figure S32), these results provide a clear explanation for the unusual $^{31}$P NMR upfield shift, namely strong electronic interactions with the adjacent aromatic rings locked in plane by the C($sp^3$) tethers, effective π back-donation from the

 © 2016 Wiley-VCH Verlag GmbH & Co. KGaA, Weinheim 

filled p orbital at oxygen into the antibonding σ* orbital at phosphorus (negative hyperconjugation), and steric effects in the phosphorus-containing six-membered rings.

The UV/Vis absorption spectrum of **1**, recorded in $CH_2Cl_2$ at RT, features three bands at 275, 298, and 310 nm whereas the emission spectrum shows two maxima at 314 and 324 nm with a quantum yield of 0.07 (Figure 3a). As corroborated by

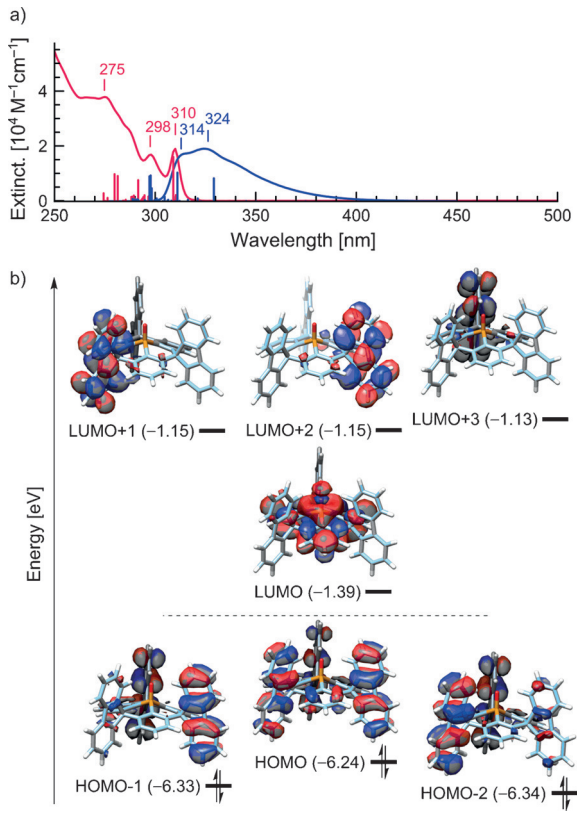


***Figure 3.*** a) Experimental UV/Vis absorption (red) and emission spectra (blue, $\lambda_{exc} = 280$ nm) in $CH_2Cl_2$ at room temperature along with the oscillator strengths (red and blue bars) obtained by TD-DFT calculations (B3PW91/def2-TZVP//PBE0/def2-TZVPP). For comparison, the computed spectra were red-shifted by 20 nm. b) Kohn–Sham molecular orbitals (DFT, PBE0/def2-QZVP).

time dependent (TD) DFT computational studies, the observed UV/Vis absorption and emission features originate from the electronic transitions from HOMO and HOMO−2 to LUMO+1, LUMO+2, and LUMO+3, respectively, without involvement of the LUMO, which is localized exclusively at the triarylphosphine oxide core (Figure 3b). Hence, all transitions are of π–π* nature and occur at the electronically independent fluorenyl moieties connected through the C($sp^3$) spiro junctions (Tables S5 and S6).

Cyclic voltammetry (CV) studies provided further insight into the electronic nature of **1** (Figure 4c). In THF, the compound undergoes a reversible reduction event at −2.85 V (all potentials are reported vs. $Fc^+/Fc$) centered at the phosphoryl moiety. Furthermore, in $CH_2Cl_2$, two independent oxidation events are observed, which were ascribed to 1) oxidation of the peripheral fluorenyl units at a half-wave potential of +1.44 V and 2) subsequent deposition of an

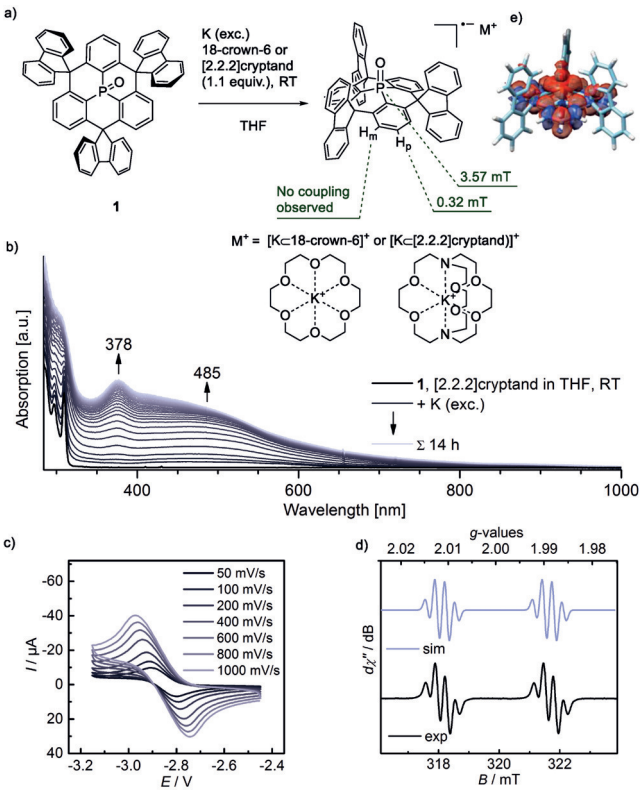


***Figure 4.*** a) Chemical reduction of **1** with potassium and 18-crown-6 or [2.2.2]cryptand. b) Evolution of the UV/Vis absorption bands upon reduction of **1**. c) Cyclic voltammogram of **1** (in THF with 0.1 M *n*-$Bu_4NPF_6$, RT, vs. $Fc/Fc^+$). d) EPR spectrum of $\mathbf{1}^{\bullet-}$ in the presence of [2.2.2]cryptand in THF at RT (black) and its simulation (blue).[27] d) Mulliken spin densities derived from DFT calculations (blue: "−", red: "+" spin density, isovalue −0.0004).

electroactive polymer film on the working electrode, as reported in the literature for other fluorenyl-containing compounds (see the Supporting Information).[25]

Treatment of **1** with an excess of potassium metal in THF in the presence of 18-crown-6 or [2.2.2]cryptand at RT resulted in a deep red solution of radical anion $\mathbf{1}^{\bullet-}$ (Figure 4a). The color change was concomitant with the emergence of a UV/Vis absorption maximum at 378 nm and a broad band centered at 485 nm, reaching saturation after 14 hours (Figure 4b). The spectral features remained largely unchanged even after prolonged treatment with an excess of potassium for three days, indicating the sufficient stability of the charged species under these conditions.[26]

As TD-DFT calculations completely failed to reproduce the UV/Vis spectrum of $\mathbf{1}^{\bullet-}$, the ZINDO/S approach with 150 roots was applied instead (Figure S33). Although the peak positions are still off by 40–60 nm, it is suggested that the absorption band around 485 nm corresponds to multiple excitations from the SOMO to the LUMO and higher lying LUMO+*n* orbitals, and that the band around 378 nm originates from multiple HOMO−*n* to LUMO+*n* excitations.

The continuous wave X-band EPR spectrum of the deep red THF solution, which was obtained by reduction of **1** with elemental potassium in the presence of [2.2.2]cryptand, recorded at RT, exhibits a sharp signal at $g \approx 2$ with a well-

 © 2016 Wiley-VCH Verlag GmbH & Co. KGaA, Weinheim 

resolved hyperfine structure (Figure 4d). The addition of [2.2.2]cryptand was found to significantly increase the resolution of the EPR spectra, most likely by interrupting the interactions between the radical anion and the potassium cation through its incorporation within the cryptand (see the Supporting Information). The observed fine structure results from hyperfine coupling of the unpaired electron with the internal $^{31}$P atom ($I = 1/2$, 100%) in addition to superhyperfine coupling to the three equivalent $^{1}$H atoms ($I = 1/2$, 99.9%) in the *para* positions of the adjacent phenyl rings. The spectrum was simulated[27] with an effective $g$ value centered at $g_{iso} = 2.0001$, a linewidth of $W_{iso} = 0.10$ mT, and hyperfine coupling constants $A(^{31}P)$ and $A(^{1}H_{para})$ of 99.9 MHz (3.57 mT) and 8.96 MHz (0.32 mT), respectively. These findings are in accordance with the EPR spectra reported previously for persistent radical anions derived from various acylphosphine oxides, in which, however, the negative charge was additionally stabilized by delocalization into the electron-withdrawing carbonyl groups.[28]

In agreement with the literature, no coupling to *meta* hydrogen atoms was observed.[9] Conclusively, the recorded EPR spectrum of $\mathbf{1}^{\bullet-}$ in the presence of [2.2.2]cryptand clearly indicates the formation of a discrete triarylphosphine oxide radical anion, with the unpaired electron spin delocalized over the phosphoryl moiety and the three adjacent phenyl rings.[29] The experimental EPR data are supported by DFT-calculated Mulliken spin densities, which confirm that only hydrogen atoms in *para* position with respect to the phosphorus atom possess unpaired spin density (Figure 4e and Table S1). The calculated $g$ value of 2.0028 and the hyperfine coupling constants (−0.25, −0.30, and −0.32 mT) for the three *para* hydrogen atoms are in satisfactory agreement with the experiment although the calculations suggest very weak coupling of the unpaired phosphorus-centered electron with the *meta* hydrogen atoms of the adjacent phenyl moieties (six values ranging from 0.03 to 0.08 mT).

Single crystals of $\mathbf{1}^{\bullet-}[K\subset 18\text{-crown-6}]^{+}$, obtained by slow diffusion of *n*-pentane into a THF solution of the compound at −35 °C under a nitrogen atmosphere, provided the very first opportunity to analyze the structural changes arising from the one-electron reduction of the triarylphosphine oxide moiety (Figure 5; for further information, see the Supporting Information). The overall geometry of the neutral parent compound **1** is largely retained in the spirocyclic scaffold of $\mathbf{1}^{\bullet-}$ (Table 1). However, significant deviations become apparent for the environment of the phosphorus center. The stronger pyramidalization of the phosphorus atom in the anionic state is illustrated by the lower sum of the C-P-C angles (308.7(6)°) for $\mathbf{1}^{\bullet-}$ than for **1** (312.8(3)°), which, in turn, leads to an increased bowl depth of 1.71 Å for $\mathbf{1}^{\bullet-}$ in comparison to 1.50 Å for the neutral compound. Despite the increased pyramidalization of $\mathbf{1}^{\bullet-}$, the intramolecular hydrogen bond length, $C(sp^2)$–H···O, remains virtually unchanged (average C52/72/92···O1 distance of 3.21(6) Å for both compounds). More importantly, upon one-electron reduction of **1**, a slight shortening of the average $P-C_{av}$ bond length from 1.762(2) Å to 1.747(4) Å and the concurrent elongation of the P–O bond from 1.4853(13) Å to 1.492(3) Å suggest delocalization of the unpaired electron over the central $(C(sp^2))_3P$–O moiety, which is in agreement with the EPR results. Comparable changes in the bonding situation have been reported for the C–O moiety in benzophenone upon one-electron reduction to the corresponding potassium ketyl radical anion, $(Ph_2CO)^{\bullet-}K^{+}$, where an elongation of the C–O bond from 1.222 Å to 1.311(5) Å and concomitant shortening of the $OC-C(sp^2)$ bond from 1.496 Å to 1.460(6) Å were observed.[30]

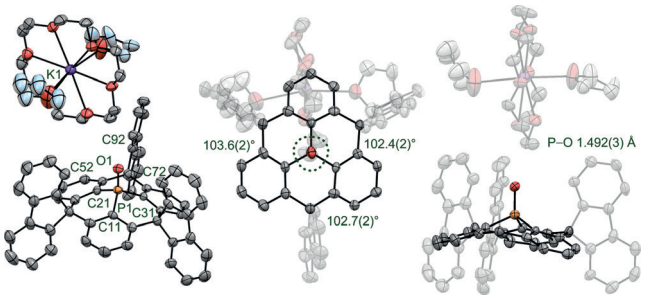


***Figure 5.*** X-ray crystal structure of $\mathbf{1}^{\bullet-}[K\subset 18\text{-crown-6}]^{+}$ and illustration of the C-P-C angles. Thermal ellipsoids set at 50% probability. C atoms of THF shown in light blue. Disordered THF molecules and H atoms omitted for clarity.

Based on the orbital picture, it can be envisaged that the addition of one additional electron to **1** to afford the corresponding radical anion should occur with an elongation of the P–O bond. Indeed, our computational studies of $\mathbf{1}^{\bullet-}$ are in good agreement with the experiment, that is, the calculated P–O bond length is 1.501 Å (exp. 1.4853(13) Å), the average P–C bond length is 1.752 Å (exp. 1.747(4) Å), and the C-P-C angles add up to 305.8° (exp. 308.7(6)°; Table 1). The SOMO of $\mathbf{1}^{\bullet-}$ strongly resembles the parent LUMO of **1**, with the unpaired electron localized on the central triarylphosphine oxide fragment (Figure 3b). The Mulliken charge distribution in $\mathbf{1}^{\bullet-}$ indicates that the phosphoryl oxygen atom becomes more negatively charged (−0.66*e*) upon reduction, while, at the same time, the the positive charge on the phosphorus atom decreases (0.39*e*) as compared to neutral compound **1** with −0.62*e* (O) and 0.50*e* (P), respectively. In accordance with this charge evolution, Mayer's bond order decreases from 1.59 in **1** to 1.48 in $\mathbf{1}^{\bullet-}$, which corresponds well with the calculated elongation of the P–O bond by 0.014 Å (Table 1, for calculated characteristics of $Ph_3PO$ and its radical anion, see the Supporting Information). In comparison to **1**, with P–bcp = 0.88 Å and O–bcp = of 0.61 Å, the AIM analysis shows that the bcp of the P–O bond in $\mathbf{1}^{\bullet-}$, with a P–bcp distance of 0.82 Å and an O–bcp distance of 0.68 Å, is shifted towards the phosphorus atom, which is also reflected in the observed shortening of the P–C bonds upon reduction.

Taken together, we have obtained a new type of organophosphorus framework by the introduction of $C(sp^3)$-hybridized spirofluorenyl bridges into the triarylphosphine oxide moiety. The incorporation of the electron-withdrawing phosphoryl moiety into a π-conjugated polycyclic framework—most likely in conjunction with the sterically shielded environment provided by the bridging fluorenyl groups—effectively stabilized the corresponding one-electron-reduced species. This phosphine oxide radical anion could thus be isolated and characterized by X-ray crystallography for the

 © 2016 Wiley-VCH Verlag GmbH & Co. KGaA, Weinheim 

very first time. On the basis of spectroscopic and computational studies, we provided fundamental insight into the structural and electronic properties of negatively charged triarylphosphine oxides, which are anticipated to be formed during electron transport in organic electronics. We believe that the described molecular design will enable the construction of phosphine oxide materials with enhanced operational stability as well as the stabilization of other heteroatom-centered radical species that are hitherto believed to be too unstable for isolation.

## Acknowledgements

This work was supported by the Deutsche Forschungsgemeinschaft (DFG) as part of SFB 953 "Synthetic Carbon Allotropes". The "Solar Technologies Go Hybrid" (SolTech) initiative of the Free State of Bavaria, the Cluster of Excellence "Engineering of Advanced Materials" (EAM) at FAU Erlangen-Nürnberg, the German Fonds der Chemischen Industrie (FCI), and the Graduate School Molecular Science (GSMS) of FAU Erlangen-Nürnberg are gratefully acknowledged for generous support. T.E.S. acknowledges support by the Bavarian Equal Opportunities Sponsorship for promoting equal opportunities for women in research and teaching.

**Keywords:** cyclization · phosphorus heterocycles · polycyclic systems · radical anions

**How to cite:** *Angew. Chem. Int. Ed.* **2016**, *55*, 13597–13601
*Angew. Chem.* **2016**, *128*, 13795–13799

[1] T. Baumgartner, *Acc. Chem. Res.* **2014**, *47*, 1613–1622.
[2] T. Leyssens, D. Peeters, *J. Org. Chem.* **2008**, *73*, 2725–2730.
[3] A. E. Reed, P. v. R. Schleyer, *J. Am. Chem. Soc.* **1990**, *112*, 1434–1445.
[4] M. Stolar, T. Baumgartner, *Chem. Asian J.* **2014**, *9*, 1212–1225.
[5] S. O. Jeon, J. Y. Lee, *J. Mater. Chem.* **2012**, *22*, 4233–4243.
[6] C. Han, Z. Zhang, H. Xu, J. Li, G. Xie, R. Chen, Y. Zhao, W. Huang, *Angew. Chem. Int. Ed.* **2012**, *51*, 10104–10108; *Angew. Chem.* **2012**, *124*, 10251–10255.
[7] N. Lin, J. Qiao, L. Duan, H. Li, L. Wang, Y. Qiu, *J. Phys. Chem. C* **2012**, *116*, 19451–19457.
[8] N. Lin, J. Qiao, L. Duan, L. Wang, Y. Qiu, *J. Phys. Chem. C* **2014**, *118*, 7569–7578.
[9] A. V. Il'yasov, Yu. M. Kargin, Ya. A. Levin, I. D. Morozova, B. V. Mel'nikov, A. A. Vafina, N. N. Sotnikova, V. S. Galeev, *Izv. Akad. Nauk SSSR Ser. Khim.* **1971**, 770–776.
[10] A. V. Ilyasov, Ya. A. Levin, I. D. Morosova, *J. Mol. Struct.* **1973**, *19*, 671–681.
[11] F. Hein, H. Plust, H. Pohlemann, *Z. Anorg. Allg. Chem.* **1953**, *272*, 25–31.
[12] A. K. Hoffmann, A. G. Tesch, *J. Am. Chem. Soc.* **1959**, *81*, 5519–5520.
[13] A. H. Cowley, M. H. Hnoosh, *J. Am. Chem. Soc.* **1966**, *88*, 2595–2597.
[14] E. Beckmann, T. Paul, *Justus Liebigs Ann. Chem.* **1891**, *266*, 1–28.
[15] A. G. Evans, J. C. Evans, D. Sheppard, *J. Chem. Soc. Perkin Trans. 2* **1976**, 1166–1169.
[16] X. Gu, H. Zhang, T. Fei, B. Yang, H. Xu, Y. Ma, X. Liu, *J. Phys. Chem. A* **2010**, *114*, 965–972.
[17] D. Hellwinkel, A. Wiel, G. Sattler, B. Nuber, *Angew. Chem. Int. Ed. Engl.* **1990**, *29*, 689–692; *Angew. Chem.* **1990**, *102*, 677–680.
[18] F. C. Krebs, P. S. Larsen, J. Larsen, C. S. Jacobsen, C. Boutton, N. Thorup, *J. Am. Chem. Soc.* **1997**, *119*, 1208–1216.
[19] M. Yamamura, T. Hasegawa, T. Nabeshima, *Org. Lett.* **2016**, *18*, 816–819.
[20] H. Tsuji, T. Inoue, Y. Kaneta, S. Sase, A. Kawachi, K. Tamao, *Organometallics* **2006**, *25*, 6142–6148.
[21] For the definition of the bowl depth, see the Supporting Information, Figure S22.
[22] A. A.-F. Khalid, *J. Crystallogr. Spectrosc. Res.* **1992**, *22*, 687–689.
[23] J. M. Casper, E. E. Remsen, *Spectrochim. Acta Part A* **1978**, *34*, 1–4.
[24] T. Kuivalainen, J. El-Bahraoui, R. Uggla, R. Kostiainen, M. R. Sundberg, *J. Am. Chem. Soc.* **2000**, *122*, 8073–8074.
[25] a) J. Rault-Berthelot, M. M. Granger, L. Mattiello, *Synth. Met.* **1998**, *97*, 211–215; b) D. Horhant, J.-J. Liang, M. Virboul, C. Poriel, G. Alcaraz, J. Rault-Berthelot, *Org. Lett.* **2006**, *8*, 257–260.
[26] Whereas a THF solution of $\mathbf{1}^{\bullet-}[K\subset 18\text{-crown-6}]^+$ kept under Ar at −35 °C was stable for several weeks, at room temperature, gradual decomposition towards EPR-silent products was observed within several days. Decomposition of $\mathbf{1}^{\bullet-}[K\subset 18\text{-crown-6}]^+$ in the solid state was indicated by rapid decoloration of the crystals upon exposure to air.
[27] F. Neese, Diploma Thesis, University of Konstanz **1993**.
[28] M. Zalibera, P.-N. Stébé, K. Dietliker, H. Grützmacher, M. Spichty, G. Gescheidt, *Eur. J. Org. Chem.* **2014**, 331–337.
[29] For the sake of comparison, EPR studies of the radical anion obtained by chemical reduction of $Ph_3PO$ were performed under the same conditions; for details, see the Supporting Information.
[30] T. A. Scott, B. A. Ooro, D. J. Collins, M. Shatruk, A. Yakovenko, K. R. Dunbar, H.-C. Zhou, *Chem. Commun.* **2009**, 65–67.

Received: June 20, 2016
Revised: August 18, 2016
Published online: September 27, 2016

 © 2016 Wiley-VCH Verlag GmbH & Co. KGaA, Weinheim 